TYPE Mini Review
PUBLISHED 12 October 2022
DOI 10.3389/fchem.2022.1039738

OPEN ACCESS

EDITED BY
Dafeng Yan,
Huazhong University of Science and Technology, China

REVIEWED BY
J. L. Xu,
Nanchang Hangkong University, China
Anmin Liu,
Dalian University of Technology, China

*CORRESPONDENCE
Chao Wang,
wangchaohit@126.com
Wu Tang,
tang@uestc.edu.cn
Hui Tang,
tanghui@uestc.edu.cn

SPECIALTY SECTION
This article was submitted to Electrochemistry,
a section of the journal
Frontiers in Chemistry

RECEIVED 08 September 2022
ACCEPTED 27 September 2022
PUBLISHED 12 October 2022

CITATION
Zhu H, Wang C, He Y, Pu Y, Li P, He L, Huang X, Tang W and Tang H (2022), Oxygen vacancies engineering in electrocatalysts nitrogen reduction reaction.
Front. Chem. 10:1039738.
doi: 10.3389/fchem.2022.1039738

Oxygen vacancies engineering in electrocatalysts nitrogen reduction reaction

Haijiang Zhu[1], Chao Wang[2]*, Yuling He[1], Yi Pu[1], Peiwen Li[1], Liang He[3], Xianglan Huang[4], Wu Tang[1]* and Hui Tang[1]*

[1]School of Materials and Energy, University of Electronic Science and Technology of China, Chengdu, China, [2]Institute of Machinery Manufacturing Technology, China Academy of Engineering Physics, Mianyang, China, [3]School of Mechanical Engineering, Sichuan University, Chengdu, China, [4]School of New Energy Materials and Chemistry, Leshan Normal University, Leshan, China

Ammonia is important, both as a fertilizer and as a carrier of clean energy, mainly produced by the Haber-Bosch process, which consumes hydrogen and emits large amounts of carbon dioxide. The ENRR (Electronchemical Nitrogen Reduction Reaction) is considered a promising method for nitrogen fixation owing to their low energy consumption, green and mild. However, the ammonia yield and Faraday efficiency of the ENRR catalysts are low due to the competitive reaction between HER and NRR, the weak adsorption of N2 andthe strong N≡N triple bond. Oxygen vacancy engineering is the most important method to improve NRR performance, not only for fast electron transport but also for effective breaking of the N≡N bond by capturing metastable electrons in the antibonding orbitals of nitrogen molecules. In this review, the recent progress of OVs (oxygen vacancies) in ENRR has been summarized. First, the mechanism of NRR is briefly introduced, and then the generation methods of OVs and their applicationin NRR are discussed, including vacuum annealing, hydrothermal method, hydrogen reduction, wet chemical reduction, plasma treatment and heterogeneous ion doping. Finally, the development and challenges of OVs in the field of electrochemical nitrogen fixation are presented. This review shows the important areas of development of catalysts to achieve industrially viable NRR.

KEYWORDS

electrocatalysts, nitrogen reduction reaction, oxygen vacancies engineering, density functional theory, synthesis methods

1 Introduction

The continued rise of the global population and excessive use of fossil fuels has led to severe environmental issues and an energy crisis. As the main constituent of air, inert nitrogen gas can be converted into ammonia, which has a large variety of applications in the industry (Galloway et al., 2008; Zamfirescu and Dincer, 2008). Nearly 80% of the ammonia produced is utilized for fertilizers, making it a significant agricultural chemical. Additionally, it can be used as a potential carrier of green fuel (Galloway et al., 2004; Christensen et al., 2006; Kitano et al., 2012; Chen et al., 2018; Li et al., 2022b). Currently, the Haber-Bosch process is used for the production of ammonia from nitrogen and hydrogen, which was invented in the early 20th century (Tanabe and Nishibayashi, 2013; Liu, 2014). However, owing to the high bond energy, lack of dipole moment, and low polarization of the molecular structure of N_2, leads to the production of Haber-Bosch process must be carried out at high pressures (150–300 ATM) and high temperatures (400–600°C), making it an energy-intensive process that accounts for about 1–2% of the world's yearly energy supplies (Chirik, 2009; van der Ham et al., 2014; Singh et al., 2017; Sun et al., 2017; Guo et al., 2018; Chen et al., 2019; Song et al., 2019). There is an urgent need for researchers to find a viable and novel method of nitrogen fixation.

Recently, many methods have been proposed for nitrogen fixation in ambient circumstances, such as biochemical catalysis, photocatalysis, and electrocatalysis (Brown et al., 2016; Milton et al., 2016; Kyriakou et al., 2017; Cao and Zheng, 2018; Cui et al., 2018; Guo W et al., 2019). Among that the ENRR has been singled out as a promising method, because of their environment friendly, low pressure and moderate temperature (Zhang et al., 2019a; Zhang et al., 2019b; Li et al., 2019; Yu et al., 2019; Lazouski et al., 2020; Yang et al., 2020). However, the completion of NRR and hydrogen evolution reaction (HER) leads to the low Faraday efficiency and low ammonia yield, which limits its application (Hao et al., 2019; Qiu et al., 2019; Zhao et al., 2019). It is well-known that high Faraday efficiency and ammonia yield are requisite conditions for industrial applications of electrocatalytic reactions. Therefore, designing and producing environmentally friendly catalysts by an efficient process with low energy consumption and minimal pollution is crucial.

Oxygen vacancies engineering strategies as an effective method to improve NRR performance can tune the electronic structure and ensure successful reaction between intermediates, resulting in excellent chemical and physical properties as well as higher activity and selectivity (Yan et al., 2017; Xu et al., 2021; Gao et al., 2022; Ji et al., 2022). In recent studies, the design of catalyst materials with OVs for electrochemical NRR has drawn significant research attention (Zhang et al., 2018; Liu et al., 2019; Yan D. F et al., 2019; Zhang S et al., 2019; He et al., 2021). Moreover, the introduction of OVs in electrocatalysts has been extensively employed in NRR because a large number of stable metal oxide catalysts provide a variety of carriers for OVs enriched with different structures (Hirakawa et al., 2017; Xu et al., 2019; Li P. S et al., 2020; Liu et al., 2021b). For instance, Han et al. thoroughly investigated the ENRR performance and catalysis mechanism of titanium dioxide with various OVs concentrations by theoretical calculations and experiments, including strict control of the annealing temperature during the preparation process (Han et al., 2019). Accordingly, In-depth exploration of the effect of OVs on ENRR is essential to guide the design of catalysts with better catalytic performance.

In this review, we provide an overview of the most recent developments in utilizing OVs for developing catalysts for electrocatalytic nitrogen fixation. First, we briefly introduce the mechanism of electrocatalytic nitrogen fixation. We additionally summarize OVs generating methods and their applications for ENRR. Finally, the future development and possible challenges of OVs in the field of ENRR are discussed.

2 NRR mechanism

The complexity of the ENRR process and the catalyst's shape, microstructure, electronic structure, and density of active sites influence the effectiveness of the catalyst. Moreover, inefficient reactions also occur since most electrons unite with protons to generate hydrogen, which is the largest competitive reaction in ENRR. Therefore, it is essential to have an in-depth understanding of the NRR process.

Adsorption and activation of N_2 on the catalyst surface, along with the associated electron conversion and proton adsorption, are the first steps in the electrochemical reduction of N_2 to NH_3. This reaction is quite difficult for the following reasons: 1) the robust triple bond of the inert N_2 molecule (Singh et al., 2017), 2) no permanent dipole, 3) a huge energy gap 10.82 eV between the highest occupied and lowest unoccupied molecular orbitals (Yan X et al., 2019), and 4) high ionization potential (15.58 eV) and low electron affinity (−1.9 eV) of the N_2 molecule (Jia and Quadrelli, 2014; van der Ham et al., 2014). Consequently, A viable NRR catalyst requires modest binding to intermediate species and a high activation capacity relative to N_2 (Wang et al., 2017).

According to the intermediates involved and energy consumption, the NRR mechanism can be theoretically separated into dissociative and associative mechanisms (Figure 1A) (Shipman and Symes, 2017). The N≡N bond is first broken by the dissociative mechanisms before hydrogenation, and then individual N atoms are adsorbed onto the catalyst surface and hydrogenated to form NH_3. The Haber-Bosch process follows the dissociative mechanism (Wan et al., 2019). The dissociative mechanism involves overcoming the high cleavage energy of the thermodynamic N≡N bond, making NRR unfavorable under ambient conditions.

In contrast to the dissociative pathway, the N≡N triple bond partially breaks in the associative mechanism, before the hydrogenation of N atoms takes place. The associative mechanism can be further classified into the distal path and the alternating path based on the sequence in which H atoms are added to the two distinct N atoms (Shipman and Symes, 2017). The distal N atom in the distal pathway first adsorbs the H atom,

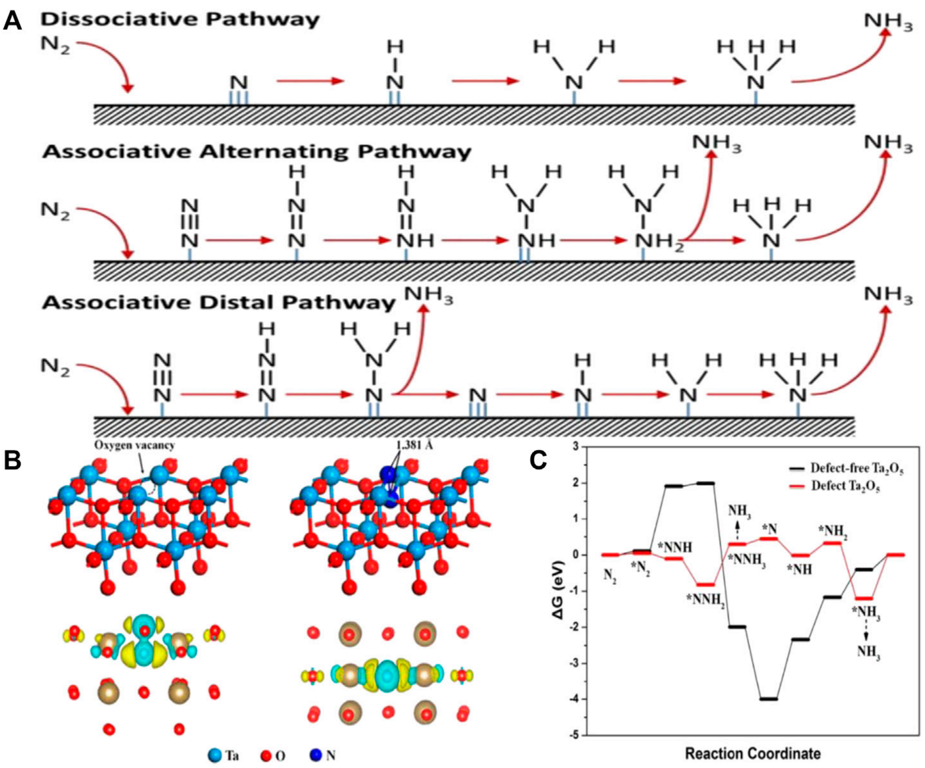

FIGURE 1
(A) Possible reaction mechanisms for the NRR to form NH_3. (Shipman and Symes, 2017) with permission from Copyright 2016 Elsevier B.V. **(B)** Model of the (001) surface of Ta_2O_5 with an O-vacancy site, the adsorption geometry of N_2 on the O-vacancy site of the Ta_2O_5 (001) surface, Side and top view of charge density difference of the N_2 adsorbed (001) surface. **(C)** DFT-calculated NRR reaction pathways and the corresponding energy changes on defect Ta_2O_5 and defect-free Ta_2O_5. (Fu et al., 2019) with permission from Copyright 2019 American Chemical Society.

and subsequently hydrogenates until forming and releasing the ammonia molecule. Then another N atom is hydrogenated to release ammonia. The alternating path uses the alternating addition of H atoms to two different N atoms until one of them converts to NH_3 and the N≡N bond is broken (Guo X et al., 2019).

In comparison to conventional catalysts, the introduction of OVs into a catalyst can increase the number of active sites for NRR by altering the electronic structure and surface properties. For example, Density functional theory (DFT) computations were carried out by Fu et al. on facets of Ta_2O_5 (001) with OVs (Fu et al., 2019). The localized electrons made the Ta ions reduce, leading to an increase in the Bader charge of the two connected Ta atoms, from 2.45 e to 2.92 and 3.00 e, as shown in Figure 1B. Meanwhile, the two partly reduced Ta atoms near the OVs swapped electrons and absorbed N_2. Their accessible d orbitals were used by the N-N π antibonding orbital to acquire electrons, which contributed to activating and adsorbing the N_2 molecule. The bond length of the successfully activated N_2 molecule increased (to 1.381 Å) due to the transfer of electrons from the Ta atom to the adsorbed N_2, which contrasts with 1.098 Å in free N_2. Moreover, the OV-containing Ta_2O_5 adsorbed N_2 more easily as shown in Figure 1C. Additionally, the hydrogenation of defect-free Ta_2O_5 had a large energy barrier. Therefore, OVs could enhance the catalyst's NRR catalytic performance.

3 Methods to generate OVs and applications in ENRR

3.1 Thermal annealing in an oxygen-deficient environment

A widely used method to generate OVs is annealing oxygen-containing compounds at high temperatures under anoxic conditions (e.g., He, N_2 and Ar) or vacuum. In the annealing process, the relative concentration of VOs can be adjusted by controlling the inert gas flow rate, final temperature, heating rate, annealing time and cooling rate

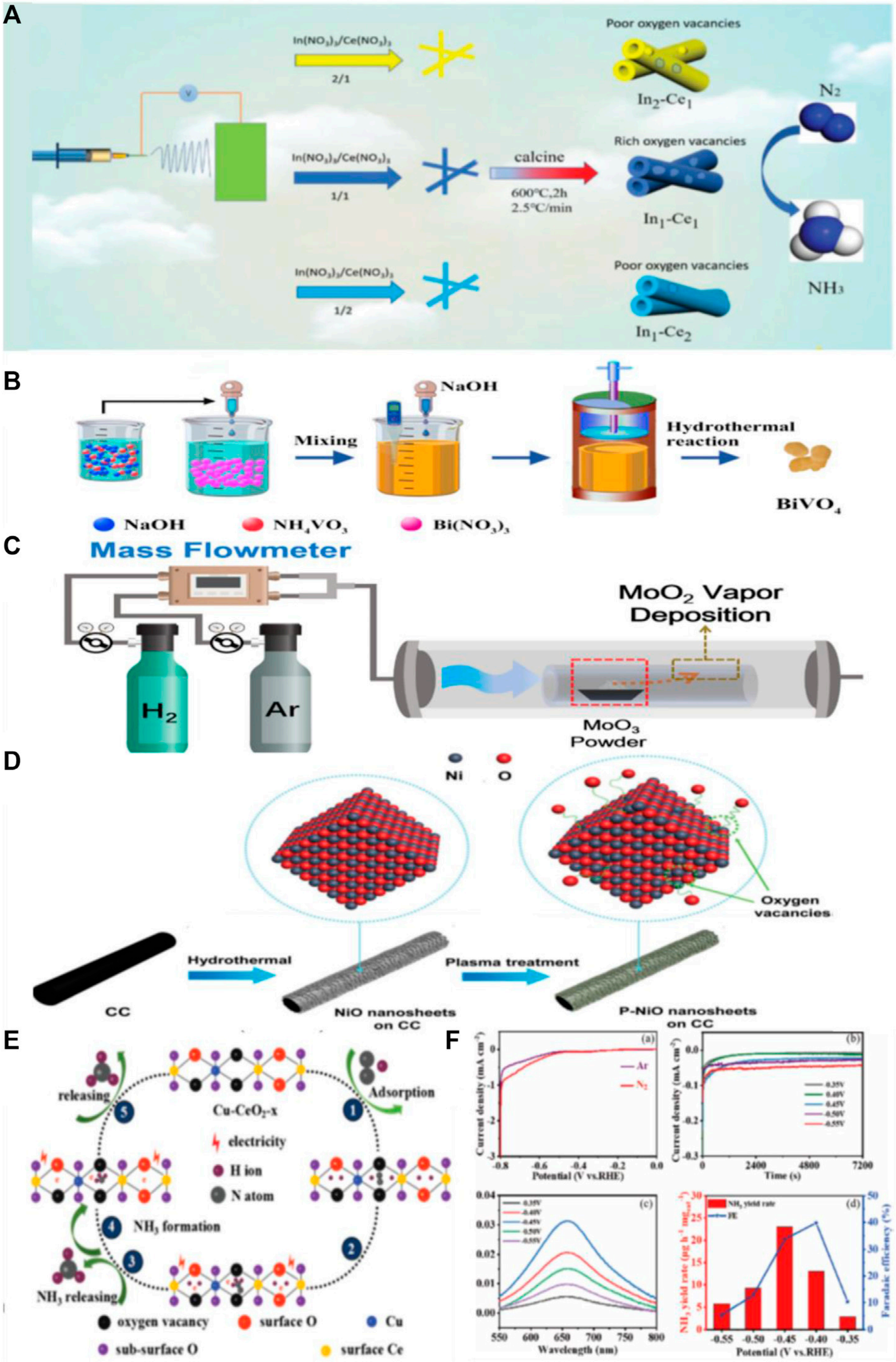

FIGURE 2
(A) The schematic diagram of the catalyst preparation and the illustration of the NRR on VO rich In_2O_{3-x}/CeO_{2-y}. (Wang et al., 2020) with permission from 2020 Royal Society of Chemistry. **(B)** Schematic illustration of the preparation of $BiVO_4$ by hydrothermal method. (Yao et al., 2019) with permission from 2018 WILEY-VCH Verlag GmbH and Co. KGaA, Weinheim. **(C)** Schematic of the preparation of MoO_2 nanosheets. (Zhang G et al., 2019) with permission from Copyright 2019 Elsevier Ltd. **(D)** Schematic illustration of the synthesis process of P–NiO/CC. (Wang Y. et al., 2019) with permission from Copyright 2020 Royal Society of Chemistry. **(E)** The proposed NRR pathway for the NH_3 synthesis on the Cu-CeO_2-3.9 catalyst. (Zhang S et al., 2019) with permission from Copyright 2019 Royal Society of Chemistry. **(F)** NRR performance of P-KNO after electrolysis at different potentials. (Fan et al., 2022) with permission from Copyright 2022 Royal Society of Chemistry.

(Sarkar and Khan, 2019; Wang L. et al., 2019; Zhu et al., 2019).

Wang et al. obtained In_2O_{3-x}/CeO_{2-y} nanotubes rich in OVs by electrostatic spinning followed by vacuum annealing (Figure 2A) (Wang et al., 2020). According to the XPS spectra, the sample In_1-Ce_1, with a raw material ratio of 1:1, showed the highest concentration of OVs. With the formation of OVs, the electrochemical properties were effectively optimized, and the kinetics of NRR and electron conduction capacity were significantly enhanced, leading to a Faraday efficiency of 16.1% and NH_3 yield of 26.1 μg h^{-1} $mg_{cat}{}^{-1}$. Luo et al. synthesized MOF-derived N-doped carbon/Co_3O_4 nanocomposites (Co_3O_4@NCs) containing OVs by vacuum annealing (Luo et al., 2019). Co_3O_4@NC-10 also showed superior NRR performance with a remarkably high NH_3 yield of 42.58 μg h^{-1} $mg_{cat}{}^{-1}$ and a Faraday efficiency of 8.5% in 0.05 M H_2SO_4, which was attributed to the synergistic interaction between the N-doped carbon and the introduced OVs.

3.2 Hydrothermal methods

Hydrothermal methods involve chemical reactions in a sealed vessel, where the temperature of the solvent is much higher than its boiling point due to the increase in autogenous pressure caused by heating. The ratio of the raw materials can be adjusted to generate OVs during the hydrothermal process. In recent years this method has been widely used since the powder does not require high-temperature calcination, thus, preventing re-agglomeration of nanoparticles and contamination.

$BiVO_4$, containing different concentrations of OVs, was synthesized by Yao et al. by a hydrothermal reaction with adjusted pH values (Figure 2B) (Yao et al., 2019). At pH = 7, $BiVO_4$ had the highest concentration of OVs. It showed excellent NRR performance, including NH_3 yields up to 8.60 μg h^{-1} $mg_{cat}{}^{-1}$, Faraday efficiency of 10.04% at −0.5 V vs RHE. Liu et al. prepared $BiVO_4/TiO_2$ nanotube ($BiVO_4$/TNT) heterojunction composites rich in OVs by a hydrothermal method (Liu et al., 2021a). With an NH_3 yield of 8.54 μg h^{-1} cm^{-2} as well as Faraday efficiency of 7.70% at −0.8 V vs RHE in 0.1 M Na_2SO_4, $BiVO_4$/TNT exhibited a remarkable performance and showed superior selectivity and high electrochemical stability.

3.3 Hydrogen reduction

Hydrogen is a strong reducing agent and is commonly used to reduce metal oxides under high temperature or high pressure to introduce OVs. The concentration of OVs in metal oxides can be controlled effectively by adjusting parameters such as pressure, temperature and gas ratios.

Zhang et al. used MoO_3 powder as the precursor and employed hydrogen reduction at 900°C for 1 h with different H_2 proportions (from 5% to 20%) in an Ar-H_2 atmosphere to obtain MoO_2 nanosheets with different OVs concentrations (Figure 2C) (Zhang G et al., 2019). DFT calculations showed that appropriately limiting OVs in the MoO_2 layer benefits the proton transfer step by selectively stabilizing N_2H^* and destabilizing $N_2H_2{}^*$ through the distal/alternate mixing path. Consequently, in comparison to MnO_2 with free OVs, the activation barrier was lowered from 1.49 eV to 0.36 eV. Fang et al. successfully prepared two-dimensional OV-TiO_2 nanosheets by annealing TiO_2 nanocrystals in H_2/Ar at different temperatures (Fang C. H et al., 2019). The OV-TiO_2-400 nanosheets remained highly stable after 12 cycles and achieved NH_3 yields of 35.6 μg h^{-1} mg^{-1}, which was 2.83 times higher than that of TiO_2 without OVs.

3.4 Wet chemical reduction

Wet chemical reduction of oxides by chemical reagents such as $NaBH_4$ can produce OVs at temperatures lower than those required for hydrogen reduction. The reduction molecule first adsorbs on the metal oxide surface and then grabs the O atom to the surface oxygen by electron transfer, thus generating OVs.

Carbon-encapsulated MoO_2 nanoparticles (MoO_2@C) with abundant OVs have been synthesized *via* a pectin-assisted hydrothermal method, followed by calcination and treatment with $NaBH_4$ solution (Du et al., 2021). MoO_2@C showed a low NH_3 yield of 2.12 μg h^{-1} mg^{-1} at −0.7 V vs RHE without treatment with $NaBH_4$ solution. However, OV-containing MoO_2@C showed a higher NH_3 yield 9.75 μg h^{-1} mg^{-1} at 0.5 V vs RHE and Faraday efficiency of 3.24% and inhibited the HER. Fang et al. synthesized OV-rich TiO_2 nanoparticles (NPs) grown *in situ* on $TiO_2/Ti_3C_2T_x$ using an ethanol-based thermal technique (Fang Y. H et al., 2019). Due to the high electrical conductivity of the $Ti_3C_2T_x$ nanosheets, electron transport was promoted and self-aggregation of TiO_2 nanoparticles was inhibited. Thus, the TiO_2 nanoparticles increased the surface specificity (SSA) of $Ti_3C_2T_x$. Moreover OVs can serve as NRR reactive sites, the $TiO_2/Ti_3C_2T_x$ exhibited an excellent NRR capability with NH_3 yields of 32.17 μg h^{-1} mg^{-1} at −0.55 V vs RHE and Faraday efficiency of 16.07% at −0.45 V vs RHE in 0.1 M HCl. DFT calculations demonstrate that the N≡N triple bond at the TiO_2 (101)/$Ti_3C_2T_x$ surface was highly activated and showed the lowest NRR energy barrier (0.40 eV) compared to untreated $Ti_3C_2T_x$ or TiO_2 (101).

3.5 Plasma treatment

Efficient and rapid generation of OVs can be achieved by plasma treatment, which involves surface etching and can be carried out at lower temperatures (Wang et al., 2018). Energetic particles, such as various kinds of plasma and high-energy protons, interact with the metal oxide surface during the plasma activation process, the surface structure is damaged, leading to the creation of OVs. The concentration of OVs can be precisely controlled by adjusting the plasma's power, pressure, gas flow, and irradiation period.

Li et al. used plasma technology to introduce OVs in NiO (Figure 2D) (Li Y. B et al., 2020). DFT calculations show that the electronic structure of NiO was modified due to the introduction of OVs, further improving its electron conduction during NRR, lowering the reaction potential barrier and suppressing side reactions. In contrast to the majority of the reported NRR catalysts, the NiO nanosheets enriched with OVs showed an excellent NH_3 yield of 29.1 μg h^{-1} mg^{-1} and Faraday efficiency of 10.8% −0.5 V vs. RHE.

3.6 Heterogeneous ion doping strategy

Heterogeneous ion doping is based on the difference in the electronegativities of intrinsic atoms, and is used to introduce defects into crystal structures and adjust the physicochemical properties of materials (Li W et al., 2020; Li et al., 2022a). For pure oxygen-containing compounds, both metallic and nonmetallic doping can create an imbalanced charge atmosphere that tends to break the long-term periodicity of the lattice oxygen in the oxide; thus, OVs are formed to maintain thermodynamic stability.

3.6.1 Metal-doping

Chu et al. tuned the NRR properties of CeO_2 by Fe doping (Fe-CeO_2) (Chu et al., 2020a). Fe doping transformed the morphology of CeO_2 from crystalline nanoparticles to partly amorphous nanosheets and significantly increased the concentrations of OVs. As a result of the abundant active sites, considerable specific surface area and high electrical conductivity, Fe-CeO_2 exhibited good catalytic activity, with an excellent NH_3 yield of 26.2 μg h^{-1} mg^{-1} (−0.5 V vs. RHE) and Faraday efficiency of up to 14.7% (−0.4 V vs. RHE).

Zhang et al. successfully prepared Cu-doped CeO_2 nanorods by a facile hydrothermal method, followed by annealing in H_2/Ar (Zhang S et al., 2019). The synthetic Cu-doped CeO_2 nanorods were designated as Cu-CeO_2-x, where x denotes the amount of Cu dopant. Cu-CeO_2-3.9 exhibited excellent electrocatalytic performance due to its large surface area of 95.2 m^2 g^{-1} and mesoporous structure, with NH_3 yields of 5.3×10^{-10} mol s^{-1} cm^{-2} and Faraday efficiencies of 19.1% at −0.45 V vs. RHE in 0.1 M Na_2SO_4, which is far beyond that of pure CeO_2 nanorods. It was found that the Ce^{3+} site in Cu-doped CeO_2 was more easily replaced by Cu^{2+} with the increase in Cu dopant concentration. As a result, the OVs around the Ce^{3+} sites decreased; conversely, the OVs surrounding the Ce^{2+} sites increased. The OVs formed around the Ce^{2+} sites promoted N_2 adsorption and activation and improved NRR performance (Figure 2E).

3.6.2 Nonmetal-doping

Chu et al. used a straightforward hydrothermal method to synthesize B-doped MnO_2 (Chu et al., 2020b). DFT calculations demonstrated that the asymmetric charge distribution brought on by the interaction between OVs and the B dopant enhanced the stability of the crucial intermediate $^*N_2H$ on MnO_2; thus, lowering the reaction energy barrier and increasing reactivity. the B-MnO_2/Carbon cloth in 0.5 M $LiClO_4$ outperformed most currently known Mn-based catalysts with an NH_3 yield of 54.2 μg h^{-1} mg^{-1} (−0.4 V vs. RHE) and Faraday efficiency of 16.8% (−0.2 V vs. RHE).

Fan et al. synthesized OV-rich P-doped potassium peroxynitrite (KNb_3O_8, abbreviated as P-KNO) by a simple solid-phase method followed by phosphorylation (Fan et al., 2022). The NH_3 yield of P-KNO was 23.01 μg h^{-1} mg^{-1} (at −0.45 V vs. RHE) and the FE was 39.77% (at −0.4 V vs. RHE) in 0.1 M Na_2SO_4 electrolyte (Figure 2F), which is twice that of unphosphorylated KNO. Additionally, due to their complementary effects, P-doping and VOs modified the electronic structure of the catalyst surface, hastening the adsorption and activation of N_2 and thus enhancing catalytic performance.

4 Summary and prospects

Ammonia is one of the most widely manufactured chemicals and has the potential for clean energy applications. However the conventional Haber-Bosch method requires significant amounts of energy and releases a considerable of greenhouse emissions. The efficient, cost-effective, and emission-free ammonia synthesis achieved from N_2 by ENRR under room temperature has attracted significant research attention. In order to substantially improve the NRR activity, developing and constructing novel effective NRR catalysts is vital.

Oxygen vacancies engineering is an effectively implemented strategy to enhance catalytic activity and selectivity of catalysts by altering the electronic state and creating additional active sites for NRR. In ENRR, OVs can alter the electron density and charge distribution of the catalyst and serve as reaction sites by adsorbing the reactants. By lowering the activation energy barrier, OVs inhibit the HER and increase the efficiency of the NRR.

Although introducing OVs to the catalyst has significantly advanced the development of NRR electrocatalysts, it is still difficult to accurately regulate OVs concentrations and the relationship between OVs and NRR performance is not well understood. In addition, OVs may introduce transition layers in the electrocatalyst during the NRR process, notably in highly acidic and alkaline electrolytes. The reaction pathways are correlated with the properties of the electrolyte and the transition layer, thus, affecting the adsorption of the intermediates and the rate-determining steps. Therefore, it is necessary to consider *in situ* characterization approaches that provide straightforward evidence and in-depth insight into the reaction mechanism. For example, *in situ* FTIR, *in situ* Raman spectroscopy and *in situ* XAFS. The performance of reported catalyst materials is unsuitable for industrial applications and needs to be further improved. We expect that improved, durable and affordable electrocatalysts for NRR can be produced by integrating experiment and theory.

Author contributions

HZ: Writing—Original Draft. CW: Conceptualization, Writing—Review and Editing. YH: Writing—Original Draft. YP: Writing—Original Draft. PL: Writing—Original Draft. LH: Review and Editing. XH: Review and Editing. WT: Conceptualization, Writing—Review and Editing. HT: Conceptualization, Writing—Review and Editing, Funding acquisition.

Funding

This research was supported by the National Science and Technology Major Project (Grant Nos. 2020YFB1506001), Department of Science and Technology of Sichuan Province (Grant Nos. 2021YFG0231, 2022YFG0258), The Sichuan Science and Technology Program (grant number: 2021JDJQ0014) and the National Natural Science Foundation of China (grant numbers: 52175444).

Conflict of interest

The authors declare that the research was conducted in the absence of any commercial or financial relationships that could be construed as a potential conflict of interest.

Publisher's note

References

Brown, K. A., Harris, D. F., Wilker, M. B., Rasmussen, A., Khadka, N., Hamby, H., et al. (2016). Light-driven dinitrogen reduction catalyzed by a CdS: nitrogenase MoFe protein biohybrid. *Science* 352 (6284), 448–450. doi:10.1126/science.aaf2091

Cao, N., and Zheng, G. (2018). Aqueous electrocatalytic N-2 reduction under ambient conditions. *Nano Res.* 11 (6), 2992–3008. doi:10.1007/s12274-018-1987-y

Chen, C., Yan, D. F., Wang, Y., Zhou, Y. Y., Zou, Y. Q., Li, Y. F., et al. (2019). B-N pairs enriched defective carbon nanosheets for ammonia synthesis with high efficiency. *Small* 15, 1805029. doi:10.1002/smll.201805029

Chen, J. G., Crooks, R. M., Seefeldt, L. C., Bren, K. L., Bullock, R. M., Darensbourg, M. Y., et al. (2018). Beyond fossil fuel-driven nitrogen transformations. *Science* 360 (6391), eaar6611. doi:10.1126/science.aar6611

Chirik, P. J. (2009). One electron at a time. *Nat. Chem.* 1 (7), 520–522. doi:10.1038/nchem.386

Christensen, C. H., Johannessen, T., Sorensen, R. Z., and Norskov, J. K. (2006). Towards an ammonia-mediated hydrogen economy? *Catal. Today* 111 (1-2), 140–144. doi:10.1016/j.cattod.2005.10.011

Chu, K., Cheng, Y. H., Li, Q. Q., Liu, Y. P., and Tian, Y. (2020a). Fe-doping induced morphological changes, oxygen vacancies and Ce3+-Ce3+ pairs in CeO2 for promoting electrocatalytic nitrogen fixation. *J. Mater. Chem. A Mater.* 8 (12), 5865–5873. doi:10.1039/c9ta14260f

Chu, K., Liu, Y. P., Cheng, Y. H., and Li, Q. Q. (2020b). Synergistic boron-dopants and boron-induced oxygen vacancies in MnO2 nanosheets to promote electrocatalytic nitrogen reduction. *J. Mater. Chem. A Mater.* 8 (10), 5200–5208. doi:10.1039/d0ta00220h

Cui, X., Tang, C., and Zhang, Q. (2018). A review of electrocatalytic reduction of dinitrogen to ammonia under ambient conditions. *Adv. Energy Mater.* 8 (22), 1800369. doi:10.1002/aenm.201800369

Du, Y. Y., He, Z. F., Ma, F. W., Jiang, Y. C., Wan, J. F., Wu, G., et al. (2021). Anionic Biopolymer assisted preparation of MoO2@C Heterostructure nanoparticles with oxygen vacancies for ambient electrocatalytic ammonia synthesis. *Inorg. Chem.* 60 (6), 4116–4123. doi:10.1021/acs.inorgchem.1c00218

Fan, S., Zhao, F., Wang, X., Wang, Q., Zhao, Q., Li, J., et al. (2022). A phosphorus-doped potassium peroxyniobate electrocatalyst with enriched oxygen vacancies boosts electrocatalytic nitrogen reduction to ammonia. *Dalton Trans.* 51, 11163–11168. doi:10.1039/d2dt01501c

Fang, C. H., Bi, T., Xu, X. X., Yu, N., Cui, Z. Q., Jiang, R. B., et al. (2019). Oxygen vacancy-enhanced electrocatalytic performances of TiO2 nanosheets toward N-2 reduction reaction. *Adv. Mater. Interfaces* 6 (21), 1901034. doi:10.1002/admi.201901034

Fang, Y. F., Liu, Z. C., Han, J. R., Jin, Z. Y., Han, Y. Q., Wang, F. X., et al. (2019). High-performance electrocatalytic conversion of N_2 to NH_3 using oxygen-vacancy-rich TiO_2 *in situ* grown on $Ti_3C_2T_x$ MXene. *Adv. Energy Mater.* 9 (16), 1803406. doi:10.1002/aenm.201803406

Fu, W., Zhuang, P., Chee, M. O., Dong, P., Ye, M., and Shen, J. (2019). Oxygen vacancies in Ta2O5 nanorods for highly efficient electrocatalytic N-2 reduction to NH3 under ambient conditions. *ACS Sustain. Chem. Eng.* 7 (10), 9622–9628. doi:10.1021/acssuschemeng.9b01178

Galloway, J. N., Dentener, F. J., Capone, D. G., Boyer, E. W., Howarth, R. W., Seitzinger, S. P., et al. (2004). Nitrogen cycles: Past, present, and future. *Biogeochemistry* 70 (2), 153–226. doi:10.1007/s10533-004-0370-0

Galloway, J. N., Townsend, A. R., Erisman, J. W., Bekunda, M., Cai, Z., Freney, J. R., et al. (2008). Transformation of the nitrogen cycle: Recent trends, questions, and potential solutions. *Science* 320 (5878), 889–892. doi:10.1126/science.1136674

Gao, K., Zhang, C., Zhang, Y., Zhou, X., Gu, S., Zhang, K., et al. (2022). Oxygen vacancy engineering of novel ultrathin Bi12O17Br2 nanosheets for boosting photocatalytic N2 reduction. *J. Colloid Interface Sci.* 614, 12–23. doi:10.1016/j.jcis.2022.01.084

Guo, C., Ran, J., Vasileff, A., and Qiao, S.-Z. (2018). Rational design of electrocatalysts and photo(electro) catalysts for nitrogen reduction to ammonia

(NH3) under ambient conditions. *Energy Environ. Sci.* 11 (1), 45–56. doi:10.1039/c7ee02220d

Guo, W., Zhang, K., Liang, Z., Zou, R., and Xu, Q. (2019). Electrochemical nitrogen fixation and utilization: Theories, advanced catalyst materials and system design. *Chem. Soc. Rev.* 48 (24), 5658–5716. doi:10.1039/c9cs00159j

Guo, X., Du, H., Qu, F., and Li, J. (2019). Recent progress in electrocatalytic nitrogen reduction. *J. Mater. Chem. A Mater.* 7 (8), 3531–3543. doi:10.1039/c8ta11201k

Han, Z. S., Choi, C., Hong, S., Wu, T. S., Soo, Y. L., Jung, Y., et al. (2019). Activated TiO2 with tuned vacancy for efficient electrochemical nitrogen reduction. *Appl. Catal. B Environ.* 257, 117896. doi:10.1016/j.apcatb.2019.117896

Hao, Y. C., Guo, Y., Chen, L. W., Shu, M., Wang, X. Y., Bu, T. A., et al. (2019). Promoting nitrogen electroreduction to ammonia with bismuth nanocrystals and potassium cations in water. *Nat. Catal.* 2 (5), 448–456. doi:10.1038/s41929-019-0241-7

He, X., Guo, H., Liao, T., Pu, Y., Lai, L., Wang, Z., et al. (2021). Electrochemically synthesized SnO2 with tunable oxygen vacancies for efficient electrocatalytic nitrogen fixation. *Nanoscale* 13 (38), 16307–16315. doi:10.1039/d1nr04621g

Hirakawa, H., Hashimoto, M., Shiraishi, Y., and Hirai, T. (2017). Photocatalytic conversion of nitrogen to ammonia with water on surface oxygen vacancies of titanium dioxide. *J. Am. Chem. Soc.* 139 (31), 10929–10936. doi:10.1021/jacs.7b06634

Ji, Y., Cheng, W., Li, C., and Liu, X. (2022). Oxygen vacancies of CeO2 Nanospheres by Mn-doping: An efficient electrocatalyst for N2 reduction under ambient conditions. *Inorg. Chem.* 61 (1), 28–31. doi:10.1021/acs.inorgchem.1c02989

Jia, H. P., and Quadrelli, E. A. (2014). Mechanistic aspects of dinitrogen cleavage and hydrogenation to produce ammonia in catalysis and organometallic chemistry: Relevance of metal hydride bonds and dihydrogen. *Chem. Soc. Rev.* 43 (2), 547–564. doi:10.1039/c3cs60206k

Kitano, M., Inoue, Y., Yamazaki, Y., Hayashi, F., Kanbara, S., Matsuishi, S., et al. (2012). Ammonia synthesis using a stable electride as an electron donor and reversible hydrogen store. *Nat. Chem.* 4 (11), 934–940. doi:10.1038/nchem.1476

Kyriakou, V., Garagounis, I., Vasileiou, E., Vourros, A., and Stoukides, M. (2017). Progress in the electrochemical synthesis of ammonia. *Catal. Today* 286, 2–13. doi:10.1016/j.cattod.2016.06.014

Lazouski, N., Chung, M., Williams, K., Gala, M. L., and Manthiram, K. (2020). Non-aqueous gas diffusion electrodes for rapid ammonia synthesis from nitrogen and water-splitting-derived hydrogen. *Nat. Catal.* 3 (5), 463–469. doi:10.1038/s41929-020-0455-8

Li, C., Mou, S., Zhu, X., Wang, F., Wang, Y., Qiao, Y., et al. (2019). Dendritic Cu: A high-efficiency electrocatalyst for N-2 fixation to NH3 under ambient conditions. *Chem. Commun.* 55 (96), 14474–14477. doi:10.1039/c9cc08234d

Li, P. S., Zhou, Z., Wang, Q., Guo, M., Chen, S. W., Low, J. X., et al. (2020). Visible-light-Driven nitrogen fixation catalyzed by Bi5O7Br nanostructures: Enhanced performance by oxygen vacancies. *J. Am. Chem. Soc.* 142 (28), 12430–12439. doi:10.1021/jacs.0c05097

Li, W., Wang, D. D., Liu, T. Y., Tao, L., Zhang, Y. G., Huang, Y. C., et al. (2022a). Doping-modulated Strain enhancing the phosphate Tolerance on PtFe Alloys for high-temperature proton Exchange Membrane fuel Cells. *Adv. Funct. Mater.* 32 (8), 2109244. doi:10.1002/adfm.202109244

Li, W., Wang, D. D., Zhang, Y. Q., Tao, L., Wang, T. H., Zou, Y. Q., et al. (2020). Defect engineering for fuel-Cell electrocatalysts. *Adv. Mater.* 32 (19), 1907879. doi:10.1002/adma.201907879

Li, W., Zhao, L., Jiang, X., Chen, Z., Zhang, Y., and Wang, S. (2022b). Confinement engineering of electrocatalyst surfaces and Interfaces. *Adv. Funct. Mater.*, 2207727–2207735. doi:10.1002/adfm.202207727

Li, Y. B., Liu, Y. P., Wang, J., Guo, Y. L., and Chu, K. (2020). Plasma-engineered NiO nanosheets with enriched oxygen vacancies for enhanced electrocatalytic nitrogen fixation. *Inorg. Chem. Front.* 7 (2), 455–463. doi:10.1039/c9qi01133a

Liu, G., Cui, Z., Han, M., Zhang, S., Zhao, C., Chen, C., et al. (2019). Ambient electrosynthesis of ammonia on a Core-Shell-Structured Au@CeO2 catalyst: Contribution of oxygen vacancies in CeO2. *Chem. Eur. J.* 25 (23), 5904–5911. doi:10.1002/chem.201806377

Liu, H. (2014). Ammonia synthesis catalyst 100 years: Practice, enlightenment and challenge. *Chin. J. Catal.* 35 (10), 1619–1640. doi:10.1016/s1872-2067(14)60118-2

Liu, Y., Deng, P. J., Wu, R. Q., Zhang, X. L., Sun, C. H., and Li, H. T. (2021b). Oxygen vacancies for promoting the electrochemical nitrogen reduction reaction. *J. Mater. Chem. A Mater.* 9 (11), 6694–6709. doi:10.1039/d0ta11522c

Liu, Y., Deng, P., Wu, R., Geioushy, R. A., Li, Y., Liu, Y., et al. (2021a). BiVO4/TiO2 heterojunction with rich oxygen vacancies for enhanced electrocatalytic nitrogen reduction reaction. *Front. Phys. (Beijing).* 16 (5), 53503. doi:10.1007/s11467-021-1067-8

Luo, S. J., Li, X. M., Zhang, B. H., Luo, Z. L., and Luo, M. (2019). MOF-derived Co3O4@NC with Core-Shell structures for N-2 electrochemical reduction under ambient conditions. *ACS Appl. Mater. Interfaces* 11 (30), 26891–26897. doi:10.1021/acsami.9b07100

Milton, R. D., Abdellaoui, S., Khadka, N., Dean, D. R., Leech, D., Seefeldt, L. C., et al. (2016). Nitrogenase bioelectrocatalysis: Heterogeneous ammonia and hydrogen production by MoFe protein. *Energy Environ. Sci.* 9 (8), 2550–2554. doi:10.1039/c6ee01432a

Qiu, W. B., Luo, Y. X., Liang, R. P., Qiu, J. D., and Xia, X. H. (2019). B4C nanosheets decorated with *in situ*-derived boron-doped graphene quantum dots for high-efficiency ambient N-2 fixation. *Chem. Commun.* 55 (51), 7406–7409. doi:10.1039/c9cc03413g

Sarkar, A., and Khan, G. G. (2019). The formation and detection techniques of oxygen vacancies in titanium oxide-based nanostructures. *Nanoscale* 11 (8), 3414–3444. doi:10.1039/c8nr09666j

Shipman, M. A., and Symes, M. D. (2017). Recent progress towards the electrosynthesis of ammonia from sustainable resources. *Catal. Today* 286, 57–68. doi:10.1016/j.cattod.2016.05.008

Singh, A. R., Rohr, B. A., Schwalbe, J. A., Cargnello, M., Chan, K., Jaramillo, T. F., et al. (2017). Electrochemical ammonia synthesis-the selectivity challenge. *ACS Catal.* 7 (1), 706–709. doi:10.1021/acscatal.6b03035

Song, P., Wang, H., Kang, L., Ran, B., Song, H., and Wang, R. (2019). Electrochemical nitrogen reduction to ammonia at ambient conditions on nitrogen and phosphorus co-doped porous carbon. *Chem. Commun.* 55 (5), 687–690. doi:10.1039/c8cc09256g

Sun, S., An, Q., Wang, W., Zhang, L., Liu, J., and Goddard, W. A., III (2017). Efficient photocatalytic reduction of dinitrogen to ammonia on bismuth monoxide quantum dots. *J. Mater. Chem. A Mater.* 5 (1), 201–209. doi:10.1039/c6ta09275f

Tanabe, Y., and Nishibayashi, Y. (2013). Developing more sustainable processes for ammonia synthesis. *Coord. Chem. Rev.* 257 (17-18), 2551–2564. doi:10.1016/j.ccr.2013.02.010

van der Ham, C. J. M., Koper, M. T. M., and Hetterscheid, D. G. H. (2014). Challenges in reduction of dinitrogen by proton and electron transfer. *Chem. Soc. Rev.* 43 (15), 5183–5191. doi:10.1039/c4cs00085d

Wan, Y., Xu, J., and Lv, R. (2019). Heterogeneous electrocatalysts design for nitrogen reduction reaction under ambient conditions. *Mater. Today* 27, 69–90. doi:10.1016/j.mattod.2019.03.002

Wang, L., Xie, X., Dinh, K. N., Yan, Q. Y., and Ma, J. M. (2019). Synthesis, characterizations, and utilization of oxygen-deficient metal oxides for lithium/sodium-ion batteries and supercapacitors. *Coord. Chem. Rev.* 397, 138–167. doi:10.1016/j.ccr.2019.06.015

Wang, P. K., Chang, F., Gao, W. B., Guo, J. P., Wu, G. T., He, T., et al. (2017). Breaking scaling relations to achieve low-temperature ammonia synthesis through LiH-mediated nitrogen transfer and hydrogenation. *Nat. Chem.* 9 (1), 64–70. doi:10.1038/nchem.2595

Wang, Y., Shi, M. M., Bao, D., Meng, F. L., Zhang, Q., Zhou, Y. T., et al. (2019). Generating defect-rich bismuth for enhancing the rate of nitrogen electroreduction to ammonia. *Angew. Chem. Int. Ed.* 58 (28), 9464–9469. doi:10.1002/anie.201903969

Wang, Z. Y., Shen, J. F., Fu, W. Z., Liao, J. W., Dong, J. C., Zhuang, P. Y., et al. (2020). Controlled oxygen vacancy engineering on In2O3-x/CeO2-y nanotubes for highly selective and efficient electrocatalytic nitrogen reduction. *Inorg. Chem. Front.* 7 (19), 3609–3619. doi:10.1039/d0qi00749h

Wang, Z., Zhang, Y., Neyts, E. C., Cao, X. X., Zhang, X. S., Jang, B. W. L., et al. (2018). Catalyst preparation with plasmas: How does it Work? *ACS Catal.* 8 (3), 2093–2110. doi:10.1021/acscatal.7b03723

Xu, H. C., Wang, Y., Dong, X. L., Zheng, N., Ma, H. C., and Zhang, X. F. (2019). Fabrication of In2O3/In2S3 microsphere heterostructures for efficient and stable photocatalytic nitrogen fixation. *Appl. Catal. B Environ.* 257, 117932. doi:10.1016/j.apcatb.2019.117932

Xu, Y. S., Liu, X. H., Cao, N., Xu, X., and Bi, L. (2021). Defect engineering for electrocatalytic nitrogen reduction reaction at ambient conditions. *Sustain. Mater. Technol.* 27, e00229. doi:10.1016/j.susmat.2020.e00229

Yan, D. F., Li, H., Chen, C., Zou, Y. Q., and Wang, S. Y. (2019). Defect engineering strategies for nitrogen reduction reactions under ambient conditions. *Small Methods* 3 (6), 1800331. doi:10.1002/smtd.201800331

Yan, D. F., Li, Y. X., Huo, J., Chen, R., Dai, L. M., and Wang, S. Y. (2017). Defect chemistry of Nonprecious-metal electrocatalysts for oxygen reactions. *Adv. Mater.* 29 (48), 1606459. doi:10.1002/adma.201606459

Yan, X., Liu, D., Cao, H., Hou, F., Liang, J., and Dou, S. X. (2019). Nitrogen reduction to ammonia on atomic-Scale Active sites under mild conditions. *Small Methods* 3 (9), 1800501. doi:10.1002/smtd.201800501

Yang, X., Ling, F., Su, J., Zi, X., Zhang, H., Zhang, H., et al. (2020). Insights into the role of cation vacancy for significantly enhanced electrochemical nitrogen reduction. *Appl. Catal. B Environ.* 264, 118477. doi:10.1016/j.apcatb.2019.118477

Yao, J. X., Boo, D., Zhang, Q., Shi, M. M., Wang, Y., Gao, R., et al. (2019). Tailoring oxygen vacancies of BiVO4 toward highly efficient Noble-metal-free electrocatalyst for artificial N-2 fixation under ambient conditions. *Small Methods* 3 (6), 1800333. doi:10.1002/smtd.201800333

Yu, J., Li, C., Li, B., Zhu, X., Zhang, R., Ji, L., et al. (2019). A perovskite La2Ti2O7 nanosheet as an efficient electrocatalyst for artificial N-2 fixation to NH3 in acidic media. *Chem. Commun.* 55 (45), 6401–6404. doi:10.1039/c9cc02310k

Zamfirescu, C., and Dincer, I. (2008). Using ammonia as a sustainable fuel. *J. Power Sources* 185 (1), 459–465. doi:10.1016/j.jpowsour.2008.02.097

Zhang, G., Ji, Q. H., Zhang, K., Chen, Y., Li, Z. H., Liu, H. J., et al. (2019). Triggering surface oxygen vacancies on atomic layered molybdenum dioxide for a low energy consumption path toward nitrogen fixation. *Nano Energy* 59, 10–16. doi:10.1016/j.nanoen.2019.02.028

Zhang, R., Guo, H., Yang, L., Wang, Y., Niu, Z., Huang, H., et al. (2019a). Electrocatalytic N-2 fixation over Hollow VO2 Microspheres at ambient conditions. *Chemelectrochem* 6 (4), 1014–1018. doi:10.1002/celc.201801484

Zhang, R., Ji, L., Kong, W., Wang, H., Zhao, R., Chen, H., et al. (2019b). Electrocatalytic N-2-to-NH3 conversion with high faradaic efficiency enabled using a Bi nanosheet array. *Chem. Commun.* 55 (36), 5263–5266. doi:10.1039/c9cc01703h

Zhang, R., Ren, X., Shi, X., Xie, F., Zheng, B., Guo, X., et al. (2018). Enabling effective electrocatalytic N2 conversion to NH3 by the TiO2 nanosheets array under ambient conditions. *ACS Appl. Mater. Interfaces* 10 (34), 28251–28255. doi:10.1021/acsami.8b06647

Zhang, S., Zhao, C., Liu, Y., Li, W., Wang, J., Wang, G., et al. (2019). Cu doping in CeO2 to form multiple oxygen vacancies for dramatically enhanced ambient N2 reduction performance. *Chem. Commun.* 55 (20), 2952–2955. doi:10.1039/c9cc00123a

Zhao, S. L., Lu, X. Y., Wang, L. Z., Gale, J., and Amal, R. (2019). Carbon-based metal-free catalysts for electrocatalytic reduction of nitrogen for synthesis of ammonia at ambient conditions. *Adv. Mater.* 31 (13), 1805367. doi:10.1002/adma.201805367

Zhu, Y. M., Liu, X., Jin, S. G., Chen, H. J., Lee, W., Liu, M. L., et al. (2019). Anionic defect engineering of transition metal oxides for oxygen reduction and evolution reactions. *J. Mater. Chem. A Mater.* 7 (11), 5875–5897. doi:10.1039/c8ta12477a